In situ magnetometry with polarized neutrons on thin magnetic films

T. Nawrath, H. Fritzsche, F. Klose, J. Nowikow, and H. Maletta*
Hahn-Meitner-Institut Berlin, Glienicker Strasse 100, D-14109 Berlin, Germany
(Received 12 April 1999)

We shall discuss perspectives opened up by using polarized neutron reflectometry as an *in situ* technique to measure the magnetization of ultrathin films not covered by a protective layer. In order to demonstrate the advantage of this method, Fe(110) films of a thickness of up to 20 Å were prepared on V(110) single crystals. In neutron measurements the absolute value of the magnetization of the films was determined precisely by a simple optical model, by fitting the spin-up and spin-down reflectivities separately. Additionally the measurements were compared with data obtained from magneto-optical Kerr magnetometry. Both techniques show that the magnetizations of the films are considerably reduced. [S0163-1829(99)12033-2]

I. INTRODUCTION

In recent years the magnetism of thin films and interfaces has received growing interest, especially after a remarkable enhancement in the magnetic moment of free magnetic layers was predicted.[1,2] It is known that protecting a thin film with a cap layer might change the magnetization of the free film. Furthermore, magnetism at interfaces is technologically interesting, since antiferromagnetically aligned bilayers or multilayers produce a giant magnetoresistance effect.[3,4]

The Fe/V system investigated in the experiments reported here has been subject to a number of experimental[5–10] as well as theoretical[11–14] studies, which, however, in the main concentrate on the magnetic moment at the (100) interface. Second, the measurements presented in these studies were either performed *in situ* in an ultrahigh vacuum chamber by methods, which do not measure the absolute magnitude of the magnetization, or the authors prepared multilayered structures and determined the magnetization at the interfaces by magnetic *ex situ* experiments.

Despite of the lack of experimental data on the Fe/V system, a number of methods exist, by which the absolute magnetization of uncovered films can be measured directly (see, e.g., Refs. 15 and 16). These methods are based on classical magnetometry, such as torsion oscillation magnetometry [TOM (Ref. 17)] or alternating gradient magnetometry [AGM (Ref. 18)].

In this paper we shall show that the magnetization of ultrathin uncovered films can also precisely be studied *in situ* with polarized neutrons. Polarized neutron reflectometry (PNR) is an established method for experiments on protected magnetic films and multilayers, and thus relates our measurements of unprotected magnetic films[19] to the studies of Felcher and co-workers[20,21] and Bland, Pescia, and Willis,[22] who performed PNR measurements on covered ultrathin films. This method is mainly based on the effect of an increasing reflectivity at the Bragg maxima which is obtained by covering the film with a cap layer of a typical thickness of 200–400 Å, while the measurements presented here were performed on a substrate, which does not have a total reflection edge for neutrons. We shall discuss the advantage of the *in situ* PNR method by presenting data on thin Fe films on V(110), which show a significant difference in the reflectivity of polarized spin-up and spin-down neutrons at sufficiently high reflectivities without covering layers being needed.

II. SAMPLE PREPARATION

All samples were prepared directly at the neutron beamline in a standard UHV chamber at a base pressure of $<10^{-10}$ mbar. This set-up is sketched in Fig. 1 with the UHV chamber containing an electron-beam evaporator and an argon-ion gun, which cleans the sample by sputtering. Furthermore, the chamber contains an AES (Auger electron spectroscopy) and a LEED (low-energy electron diffraction) system. As shown in Fig. 1, the sample is positioned above the electron-beam evaporator, where it can also be characterized by AES and LEED. For the neutron measurements the sample was moved into the quartz cylinder, where it was studied by a neutron beam.

Before the epitaxial iron films were prepared, the V(110) single crystal was cleaned repeatedly during several sputtering and annealing cycles, using argon ions of 700 eV during the sputtering and a temperature of 1400 K during the annealing cycles in order to recrystallize the surface. This process was repeated for 120 h until the contamination of the surface was below the detection limit of our Auger spectrometer, i.e., below 2% of a monolayer for sulfur or carbon and

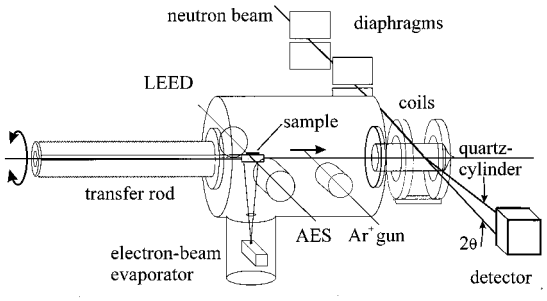

FIG. 1. Experimental setup of the *in situ* polarized neutron reflectivity (PNR) method with the UHV preparation chamber. The Helmholtz coils provide a horizontal magnetic field directed perpendicular to the neutron beam, which is necessary for this method to saturate the magnetization of the film sample.

below 5% for oxygen, as the oxygen transition coincides partly with the vanadium LMM transition. No other contamination was detected during the sputtering and annealing cycles. Before evaporation of the iron the single crystal was covered with a vanadium layer of 10 Å, which resulted in a well-ordered surface with a typical terrace width of 89 Å in the [001] and 50 Å in the $[1\bar{1}0]$ direction, respectively.[23]

The films were evaporated by molecular-beam epitaxy (MBE) at a rate of 0.07 Å/s at a sample temperature of 320 K. The thickness of the films was controlled by a calibrated quartz balance during evaporation. The conditions created a special growth mode for iron films with a collapse in the island size at a film thickness $t_{\mathrm{Fe}}=4$ Å, and an island size of 21 Å in [001] and 9 Å in $[1\bar{1}0]$. Above $t_{\mathrm{Fe}}=10$ Å the island size of the iron films increases again to values of 30 Å in [001] and 20 Å in $[1\bar{1}0]$. It is important to mention that this behavior is not connected to a Vollmer-Weber (island) growth as the AES intensities of iron and vanadium measured dependently of the iron thickness show a coverage that is typical for a Frank-van der Merwe (layer) growth, which makes the study of the magnetic behavior of films particularly interesting. For a more detailed discussion of the preparation and structure of the films see Ref. 23.

III. EXPERIMENTAL SETUP

The experiments were performed with the standard setup of the reflectometer V6 (Ref. 24) at the Hahn-Meitner-Institut Berlin, that was adjusted to a wavelength of 4.66 Å. It uses a graphite monochromator, a liquid-nitrogen-cooled Be filter, a set of two diaphragms, and a polarizing supermirror,[25] which create a polarized, monochromated, and well collimated neutron beam.

For the *in situ* experiment, an UHV preparation chamber was placed into the neutron beam of the reflectometer as sketched in Fig. 1. The angle θ between the incoming neutron beam and the sample surface was adjusted by a precision rotary feedthrough at the UHV preparation chamber. The neutron intensity transmitted through the quartz cylinder amounted to 90%. The measurement position was also surrounded by Helmholtz coils outside the chamber providing a horizontal magnetic field perpendicularly directed to the neutron beam ($H_{\mathrm{max}}=1200$ G).

The neutron detector was a two-dimensional position sensitive scintillation detector[26] with a lateral resolution of 50 μm. The angle of 2θ was determined precisely by the distance between the reflected and the transmitted beam. To perform measurements at low temperatures the transfer rod (Fig. 1) was flooded with liquid helium and the sample was put into a copper box, which was in contact with the helium bath. Since the cooling also resulted in a lower base pressure of 4×10^{-11} mbars, the sample holder was cooled with liquid He during all PNR measurements.

IV. EXPERIMENTAL METHOD

In what is to follow we shall in detail describe the method of *in situ* magnetometry with polarized neutrons on thin films. For reflectometry the interfaces of the films were arranged perpendicularly to the scattering vector $\mathbf{q}=\mathbf{k}_f-\mathbf{k}_i$ with $\mathbf{k}_i$ and $\mathbf{k}_f$ as the incoming and outgoing neutron wave vector (and $k=2\pi/\lambda$). Thus the interaction with the film is reduced to a one-dimensional problem, which can be described as an optical potential V_j (Fermi pseudopotential) for grazing incidences:

$$V_j=\frac{2\pi\hbar^2}{m}N_j b_j-\boldsymbol{\mu}\mathbf{B}_j, \tag{1}$$

where m is the neutron mass, N_j the atomic density, b_j the nuclear scattering length of the material, μ the magnetic moment of the neutron, and $\mathbf{B}_j$ the magnetic induction, whereas the index j refers to the layer number.

The first term in Eq. (1) results from the interaction of the neutron and the nucleus, while the second term results from the interaction of the neutron and the magnetization of the sample. Both terms are of the same order of magnitude (see, e.g., Ref. 27 for some specific values) and the second term can also be given as a scattering length density $N_j b_j^m$, where b_j^m is directly proportional to the magnetic moment μ_j per atom, with $b_j^m=c\mu_j$ and $c=2.695$ fm/Bohr magneton. Here $+N_j b_j^m$ denotes the magnetization parallel to the neutron spin, while $-N_j b_j^m$ denotes the antiparallel configuration.

In our setup the polarized neutrons were aligned parallel or antiparallel to the sample field by a Mezei-type flipping coil, while the magnetization of the sample remained in direction of the sample field perpendicular to the neutron beam. Please note that it is a characteristic of neutron scattering that a magnetization parallel to the scattering vector has no effect on the potential V_j,[28] and thus only the in-plane component of the magnetization is measured. To determine this component precisely, the magnetization of the sample has to be saturated in direction of the applied field. 1200 G were applied which is sufficient according to our magneto-optical Kerr effect (MOKE) measurements. A 90% polarization of the neutron beam was gained at the sample position, and taken into account for the data evaluation.

According to Eq. (1), the perpendicular component of the wave vector k in the jth medium is

$$k_j^{\perp}=\sqrt{\frac{2m}{\hbar^2}(E-V_j)}, \tag{2}$$

with $E=\hbar^2(k\sin\theta)^2/2m$. Here the reflectivity of the sample can be calculated by the Schrödinger equation. In the simulations presented here the Schrödinger equation is solved by a program which is based on the Parratt formalism[29,30] and was written by de Haan.[31] Please note that all simulations shown in this section in Figs. 2–4 were performed with a neutron polarization of 100% in contrast to our experimentally achieved polarization of 90%.

Contrary to x rays, the nuclear scattering length b of neutrons is not proportional to the atomic number. For some elements small or even negative scattering length values can occur. The scattering length density of vanadium is Nb$=-27.6\,\mu\mathrm{m}^{-2}$.

This effect can be used to measure the magnetization of thin films as shown in the simulations of the neutron reflectivity in Fig. 2(a), where it is assumed that the vanadium substrate is covered by a 20-Å-thick Fe film with bulk magnetic moment. This results in a distinct splitting of the spin-up and spin-down reflectivities with a higher reflectivity

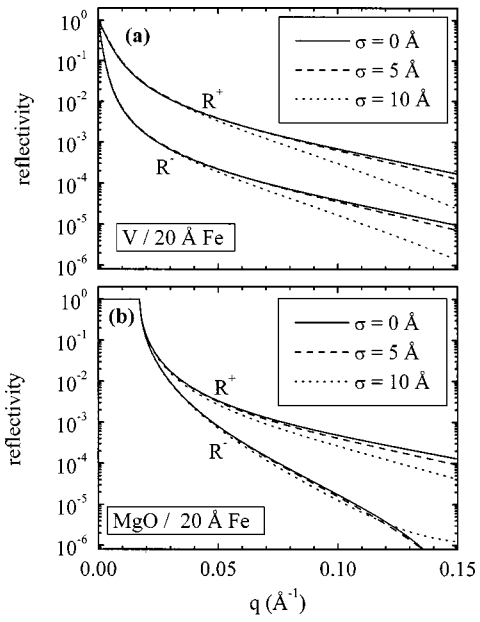

FIG. 2. (a) Simulations of the spin-up (R^+) and spin-down reflectivities (R^-) of a 20-Å-thick Fe film on a vanadium substrate with different roughnesses as indicated in the figure. The spin-up reflectivities are always represented by the upper branches. (b) The same simulations with 20-Å Fe on a MgO substrate.

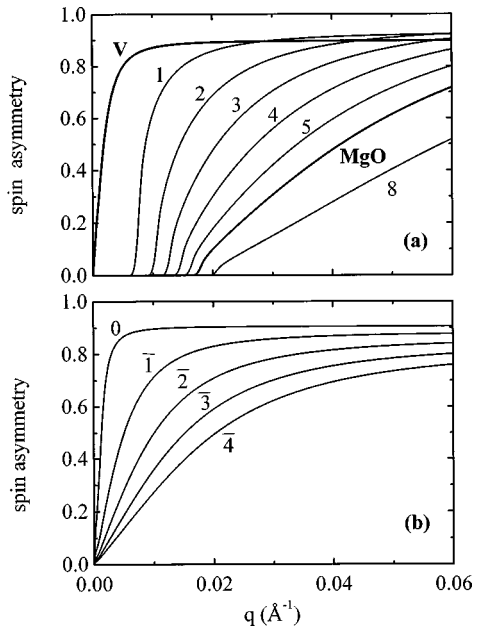

FIG. 3. (a) Simulations of the spin asymmetry of a 20-Å-thick Fe film on V and MgO substrates (thick lines with $Nb_v = -27.6\ \mu m^{-2}$ and $Nb_{MgO} = 597.2\ \mu m^{-2}$, respectively). In addition, simulations for various substrates are shown, with a scattering length density Nb of 100, 200, 300, 400, 500, and 800 μm^{-2} for the graphs numbered 1, 2, 3, 4, 5, and 8. (b) Simulations with Nb $= 0, -100, -200, -300$, and $-400\ \mu m^{-2}$ for the graphs numbered 0, $\overline{1}$, $\overline{2}$, $\overline{3}$, and $\overline{4}$.

for the spin-up signal. For comparison a reflectivity profile of a 20-Å Fe layer on MgO is simulated in Fig. 2(b) with the scattering length density of 597.2 μm^{-2} for MgO, a substrate that is widely used for the epitaxy of iron. Due to the higher Fermi pseudopotential [Eq. (1)] of the iron film for spin-up neutrons the spin-up branch shows higher reflectivities in both simulations.

The interfacial roughness is another parameter which is generally important for reflectivity measurements. It is defined as the averaged deviation from the mean interface position, $\sigma = \sqrt{\overline{(z-\overline{z})^2}}$, and is simulated by a Debye-Waller factor. Our simulations in Fig. 2 show that this parameter has no influence on the reflectivity in the very low q range. This is advantageous for applications of the PNR method for a quantitative determination of the magnetization of the film (see below).

For both substrates the reflectivities decrease relatively rapidly and proportionally to q^{-4} for larger scattering vectors. However, only for vanadium a distinct splitting of the spin-up and spin-down signal occurs at reflectivities above 10^{-3}, a value that can easily be measured with neutrons. Compared to this, the splitting for MgO is much smaller even for smaller reflectivities.

It is also important to mention that in the q range investigated here the neutrons are not sensitive to the detailed magnetization depth profile of the film, and thus only the average magnetization of the sample is measured. In order to study a magnetization profile of the film much higher q values would be required.

In the next section we should like to introduce the spin asymmetry in order to describe our experiments:

$$S = \frac{R^+ - R^-}{R^+ + R^-}, \tag{3}$$

where R^+ is the spin-up and R^- the spin-down reflectivity. In Fig. 3(a) the calculated spin asymmetries of 20-Å Fe layers on V and MgO are plotted (thick lines). The vanadium substrate shows a rapid increase of S at low q values, which is in agreement with the splitting of the spin-up and the spin-down signal in Fig. 2(a). Contrary to this, S increases much more moderately behind the total reflection edge of the MgO substrate. This can be explained by a higher (inner) reflectivity coefficient at the Fe/MgO interface, which overlaps the spin dependent reflectivity of the magnetic film. The lines numbered 1–5 and 8 in Fig. 3(a) are simulations with a scattering length density of the substrate of 100, 200, 300, 400, 500, and 800 μm^{-2}. Here the transition from V to MgO substrate materials can be studied.

Since a rapidly increasing spin asymmetry is the main condition under which magnetic *in situ* measurements can be performed, the substrate scattering length density cannot be higher than 200 μm^{-2}.

In Fig. 3(b) the spin asymmetry for negative scattering length densities is plotted with 0, $\overline{1}$, $\overline{2}$, $\overline{3}$, $\overline{4}$ for values of 0, -100, -200, -300, $-400\ \mu m^{-2}$ for Nb. Thus *in situ* PNR requires a minimum scattering length density of $-100\ \mu m^{-2}$. At lower scattering length densities the reflectivity coefficient of the film/substrate interface increases, which again leads to reduced splitting near $q = 0\ Å^{-1}$, and consequently the spin asymmetry increases more moderately at Nb values lower than $-100\ \mu m^{-2}$. Since in our experiments we access a typical maximum scattering vector q of only 0.02 $Å^{-1}$, the vanadium substrate is almost ideally suited to gain high spin asymmetries.

The dependence of the simulated spin asymmetry S on the

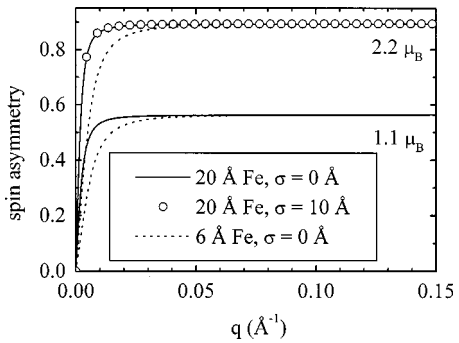

FIG. 4. Spin asymmetry simulated for 6- and 20-Å Fe (with different roughness) on vanadium. The simulations are performed with the magnetic moment of bulk iron ($2.2\mu_B$ per atom), and with $1.1\mu_B$ per atom. It is remarkable that the saturation value of the spin asymmetry is independent of the thickness and roughness of the film.

magnetization of iron on vanadium is shown in Fig. 4 for 6-Å Fe without roughness (dotted line), 20-Å Fe without roughness (solid line), and 20-Å Fe with roughness of $\sigma = 10$ Å (open circles). The upper functions are simulated with a magnetic moment of $2.2\mu_B$/iron atom, which is equivalent to the bulk magnetic moment, and the lower functions show simulations with a magnetic moment of $1.1\mu_B$/iron atom. It is important to note that the saturation value of S only depends on the average magnetic moment of the film, but not on the other two parameters, the thickness or the roughness of the film.

The thickness of the film mainly influences the magnitude of the reflectivity, and results in a higher mean reflectivity of the spin-up and spin-down signal for thicker films (see, e.g., Fig. 5). Therefore the (mean) reflectivity can be fitted by the film thickness, while the spin asymmetry determines the averaged magnetic moment of the film. Thus the two main parameters, i.e., thickness and magnetization of the film, can be fitted independently, and an absolute value is obtained for the film thickness, which can also be compared to AES intensities from Fe-LMM and V-LMM transitions (see Fig. 7, and also Ref. 23).

V. EXPERIMENTAL RESULTS

In Figs. 5(a)–(c) the measured neutron reflectivities of iron films deposited on V(110) with a thickness of 6, 10, and 19.5 Å are presented. The spin-up reflectivities are plotted as up and the spin-down as down triangles, respectively. The Fe films of a thickness of 6 and 10 Å were measured at 80 K, whereas the 19.5-Å film was measured at $T = 110$ and 300 K. The results are plotted as filled and open triangles. The spin asymmetries are shown in Fig. 6.

The data were fitted with two free parameters: the thickness and the magnetic moment of the film. The best fits are shown as solid lines and the dotted lines are simulations with the bulk magnetic moment of $2.2\mu_B$ per iron atom. A neutron polarization of 90% were taken into account in these simulations.

Figure 5 shows that for all measurements best fits are obtained at reduced magnetic moments. Values of 1.8 and $1.3\mu_B$/iron atom are obtained for $t_{\mathrm{Fe}} = 19.5$ and 10 Å, respectively, while the magnetization vanishes at a film thickness

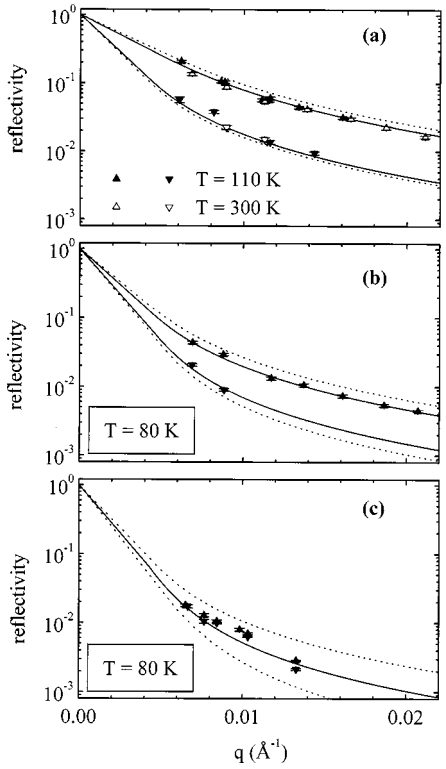

FIG. 5. PNR measurements of iron films of various thicknesses of 19.5, 10, and 6 Å on V(110) are shown in parts (a), (b), and (c), respectively. The reflectivities of the spin-up neutrons are given as up triangles, the spin-down reflectivities as down triangles. The simulations with the magnetic moment of bulk iron are shown for comparison as dotted lines, whereas the best fits are shown as solid lines. The best fits are performed with a magnetic moment per atom of 1.8, 1.3, and $0\mu_B$, respectively.

of 6 Å. At a film thickness of 19.5 Å no dependence on the measuring temperature was observed. Both measurements are best fitted with a moment of $1.8\mu_B$/atom. Hence the observed reduction in the magnetization cannot be explained by a temperature-dependent effect caused by a lower Curie temperature of the thin film.

We should like to mention that all samples were checked for surface contamination before and after the PNR measurements by Auger electron spectroscopy (AES). The two spectra of an Fe film thickness of 19.5 Å shown in Fig. 7 reveal that the samples are free of contamination. The upper spectrum (a) in Fig. 7 was obtained directly after the film was prepared. On the left-hand side of the three Fe-LMM peaks (at 598, 651 and 703 eV) there are the LMM peaks of the vanadium substrate and the Fe transition at low energies (47 eV). In Fig. 7(b) a spectrum of the same film after a typical measuring time of 12 h is presented. Neither before nor after the PNR measurements do any other but the iron and vanadium Auger transitions peaks indicate surface contamination.

The magnetization of the film was additionally investigated by magneto-optical Kerr effect (MOKE) measurements. These experiments were carried out on iron wedges which were prepared under the same conditions as the samples for the *in situ* PNR measurements. The inclination of the wedges amounted to 0.6 Å/mm, while the diameter of the laser spot was ≈0.3 mm. The measurements were also performed *in situ* at $T = 300$ K with *s*-polarized light in a

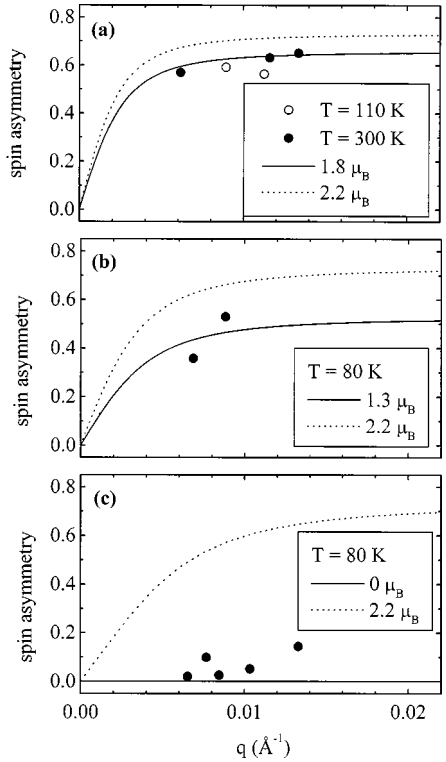

FIG. 6. The spin asymmetry of Fe films on V(110) as calculated from the reflectivity data shown in Fig. 5. (a) V(110)/19.5 Å Fe, (b) V(110)/10 Å Fe, (c) V(110)/6 Å Fe. The simulations with the magnetic moment of bulk iron are shown for comparison as dotted lines, whereas the best fits are shown as solid lines.

longitudinal geometry, sensitive to the in-plane component of the magnetization. The source was a He-Ne laser ($\lambda = 632.8\,\mathrm{nm}$), the amplitude of which was modulated with a frequency of 100.24 kHz, by a subsequent arrangement of a polarizer, a photoelastic modulator, and a second polarizer.

In Figs. 8(a) and (b) two hysteresis loops of the MOKE measurements with an iron thickness of 7 and 6 Å are plotted. A clear magnetic signal occurs at $t_{\mathrm{Fe}}=7$ Å. This signal is not detectable at $t_{\mathrm{Fe}}=6$ Å, which is in agreement with the PNR results shown in Fig. 5(c).

In Fig. 9 the total size of the Kerr rotation [that means the jump in the rotation as shown in Fig. 8(a)] is plotted as circles versus the iron thickness. This value is proportional to the magnetization in the thin-film limit, whereas the proportionality factor depends on the experimental setup (angle of

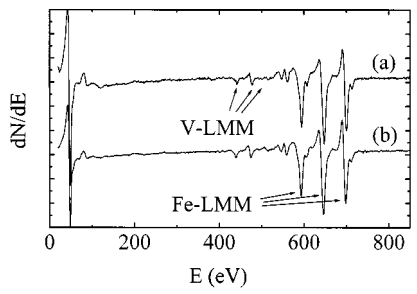

FIG. 7. Auger electron spectroscopy (AES) pattern of the 19.5 Å thick Fe film on V(110) (the same as shown in Fig. 5a). Part (a) is the spectrum measured before, part (b) after the PNR experiment.

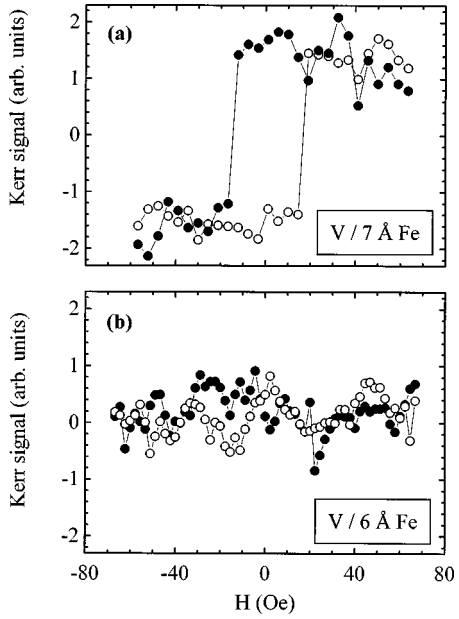

FIG. 8. (a) Magneto-optical Kerr (MOKE) hysteresis loop of the 7-Å-thick Fe film on V(110). (b) Kerr hysteresis loop of 6-Å Fe on V(110).

incidence, *s* or *p* polarization of the light, etc.) and on the optical constants of the film and the substrate. In this case it is not trivial to make a quantitative statement with respect to the magnetization. (For *ab initio* calculations of the Kerr rotation of 3*d* transition metal materials see, e.g., Ref. 32.)

From the results of the PNR measurements, the magnetic moment per atom multiplied by the iron thickness was derived and also plotted in Fig. 9 (squares) versus the iron thickness. This product is proportional to the magnetization of the film and increases with increasing film thicknesses. Therefore the Kerr data can be adjusted to the PNR data by applying a multiplication factor specific to the setup of the MOKE experiment. As shown in Fig. 9, both sets of data are on the same line, which is parallel to the dotted line intersecting with the origin with a slope of $2.2\mu_B$ for bulk iron. The shift between those two lines determines the magnetic offset of the thin film, which is negative here and amounts to -4 Å. The observed offset is therefore independent of the film thickness. This means that the magnetization of the thin

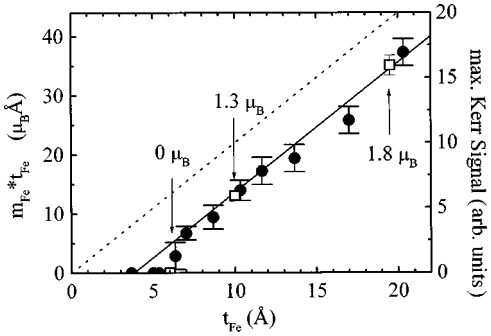

FIG. 9. Magnetization values of the iron films on V(110) due to the PNR measurements are plotted as the product of the magnetic moment per atom times the iron thickness t_{Fe} (squares) versus t_{Fe}. In the same diagram the maximum Kerr signals obtained on a similarly prepared Fe wedge are plotted as full circles.

Fe films on V(110) leads to a reduced magnetic moment which is equivalent to a magnetically dead layer with a thickness of 4 Å. As already pointed out, this statement applies to the in-plane component of the magnetization, which was the only component measured by neutron reflectometry. The reduced magnetization observed may (at least partially) also be caused by an antiferromagnetically polarized substrate. This problem will be discussed in detail in a follow-up paper, in which further experimental results will also be presented.

VI. DISCUSSION

The simulations shown in Figs. 2–4 allow for the following main conclusions:
(i) There are two parameters which are important for the fitting of the reflectivity of single ultrathin films: the thickness and the magnetization of the film. The thickness has the same influence on the reflectivity of the spin-up and the spin-down neutrons and leads to higher reflectivities for thicker films. Consequently, the averaged reflectivity increases with the thickness of the films. On the other hand, if a film has a large magnetic moment, the spin-up and the spin-down reflectivity curves always split widely. (ii) The spin asymmetry S can be interpreted as a direct measure of the averaged in-plane magnetization. It is important to note that the saturation value of S does not depend on the thickness of the film. (iii) The measurements are independent of the interfacial roughness, because they were performed at very low q values. (iv) The spin asymmetry decreases at higher positive as well as at higher negative scattering length densities of the substrate. This can be explained by the high reflectivity of the substrate overlapping the spin dependence of the magnetic film. For the *in situ* magnetometry with PNR the best range for the scattering length density of the substrate varies from -100–200 $\mu\mathrm{m}^{-2}$.

In Fig. 9 the magnetic data obtained from the PNR and the MOKE measurements are compared. (This is justified, as the measurements presented in Fig. 5(a) show no temperature dependence of the magnetization at $T=300$ and 110 K.) Here the PNR and MOKE measurements show consistent results.

In summary our first measurements by the *in situ* PNR method demonstrate that it is indeed possible to precisely determine the magnetization of ultrathin uncovered films *in situ* with polarized neutrons on a reflectometer. In the experiments described here a precision of $0.05\mu_B$/atom was achieved for iron films of a thickness <20 Å. The precision mainly depends on the neutron flux and can hence be increased by a more intense neutron source. In our next experiments a precision gain is to be expected from a factor of two more efficient position sensitive detector.

Compared to other *in situ* methods, the high sensitivity and the possibility to determine the absolute value of the magnetization of thin films are the main advantages of the PNR method. It is shown that the precise knowledge of both the film thickness and the interfacial roughness are not required in order to determine the absolute value of the magnetization from the PNR data. Additionally, there are only few restrictions with respect to the sample geometry, i.e., that the neutrons have to be reflected from the sample at a small angle. Due to the high transmission probability of the neutrons for the most materials, these conditions are easy to provide.

ACKNOWLEDGMENTS

This work was funded by the Verbundforschung of BMBF under Grant No. 03-MA4 HMI-1. The authors are indebted to K. Diederichsen for editing the manuscript.

*Author to whom correspondence should be addressed. FAX: +49-30-8062-2523. Electronic address: maletta@hmi.de

[1] C. L. Fu, A. J. Freeman, and T. Oguchi, Phys. Rev. Lett. **54**, 2700 (1985).
[2] S. Blügel, Phys. Rev. Lett. **68**, 851 (1992).
[3] P. Grünberg, R. Schreiber, Y. Pang, M. B. Brodsky, and H. Sowers, Phys. Rev. Lett. **57**, 2442 (1986).
[4] M. N. Baibich, J. M. Broto, A. Fert, F. Nguyen Van Dau, F. Petroff, P. Eitenne, G. Creuzet, A. Friederich, and J. Chazelas, Phys. Rev. Lett. **61**, 2472 (1988).
[5] T. G. Walker and H. Hopster, Phys. Rev. B **49**, 7687 (1994).
[6] P. Fuchs, K. Totland, and M. Landolt, Phys. Rev. B **53**, 9123 (1996).
[7] L.-C. Duda, P. Isberg, S. Mirbt, J.-H. Guo, B. Hjörvarsson, J. Nordgren, and P. Granberg, Phys. Rev. B **54**, 10 393 (1996).
[8] M. A. Tomaz, W. J. Antel, Jr., W. L. O'Brien, and G. R. Harp, J. Phys.: Condens. Matter **9**, L179 (1997).
[9] P. Poulopoulos, P. Isberg, W. Platow, W. Wisny, M. Farle, B. Hjörvarsson, and K. Baberschke, J. Magn. Magn. Mater. **170**, 57 (1997).
[10] H. Fritzsche, T. Nawrath, H. Maletta, and H. Lauter, Physica B **241-243**, 707 (1998).
[11] A. Vega, A. Rubio, L. C. Balbas, J. Dorantes-Davila, S. Bouarab, C. Demangeat, A. Mokrani, and H. Dreyssé, J. Appl. Phys. **69**, 4544 (1991).
[12] A. Vega, L. C. Balbás, H. Nait-Laziz, C. Demangeat, and H. Dreyssé, Phys. Rev. B **48**, 985 (1993).
[13] P. Martin, A. Vega, C. Demangeat, and H. Dreyssé, J. Magn. Magn. Mater. **148**, 177 (1995).
[14] R. Coehoorn, J. Magn. Magn. Mater. **151**, 341 (1995).
[15] H. Fritzsche, H.-J. Elmers, and U. Gradmann, J. Magn. Magn. Mater. **135**, 343 (1994).
[16] C. Turtur and G. Bayreuther, Phys. Rev. Lett. **72**, 1557 (1994).
[17] H. J. Elmers and U. Gradmann, Appl. Phys. A: Solids Surf. **51**, 255 (1990).
[18] P. J. Flanders, J. Appl. Phys. **63**, 3940 (1988).
[19] T. Nawrath, H. Fritzsche, F. Klose, J. Nowikow, C. Polaczyk, and H. Maletta, Physica B **234-236**, 505 (1997).
[20] G. P. Felcher, K. E. Gray, R. T. Kampwirth, and M. B. Brodsky, Physica B & C **136**, 59 (1986).
[21] Y. Y. Huang, C. Liu, and G. P. Felcher, Phys. Rev. B **47**, 183 (1993).
[22] J. A. C. Bland, D. Pescia, and R. F. Willis, Phys. Rev. Lett. **58**, 1244 (1987).
[23] T. Nawrath, H. Fritzsche, and H. Maletta, Surf. Sci. **414**, 209 (1998).

[24] F. Mezei, R. Golub, F. Klose, and H. Toews, Physica B **213&214**, 898 (1995).
[25] T. Krist, K. Pappas, T. Keller, and F. Mezei, Physica B **213&214**, 939 (1995).
[26] C. Rausch, M. Dietze, J. Felber, J. Hofmann, and B. Schillinger, J. Neutron Res. **3**, 171 (1996).
[27] V. F. Sears, Neutron News **3**, 26 (1992).
[28] S. W. Lovesey, *Theory of Neutron Scattering from Condensed Matter* (Clarendon, Oxford, 1986).
[29] L. G. Parratt, Phys. Rev. **95**, 359 (1954).
[30] G. P. Felcher, R. O. Hilleke, R. K. Crawford, J. Haumann, R. Kleb, and G. Ostrowski, Rev. Sci. Instrum. **58**, 609 (1987).
[31] V. O. de Haan and G. G. Drijkoningen, Physica B **198**, 24 (1994).
[32] H. Ebert, Rep. Prog. Phys. **59**, 1665 (1996).